



Theoretical analysis for thermal consolidation of marine sediments with depth variability subjected to time-dependent loading and heating

Ming-Jun Hu^{a,b}, Wei-Qiang Feng^{a,c,*}, Jun Yang^b

^a Department of Ocean Science and Engineering, Southern University of Science and Technology, Shenzhen, China

^b Department of Civil Engineering, The University of Hong Kong, Hong Kong, China

^c Southern Marine Science and Engineering Guangdong Laboratory (Guangzhou), China

ARTICLE INFO

Handling Editor: Prof. A.I. Incecik

Keywords:

Analytical solution
Thermal consolidation
Time-dependent loading
Marine sediments

ABSTRACT

Because the spatial distribution of energy is restricted, many energies geotechnics would build on marine sediments and the resulting thermal consolidation would pose an inevitable threat to the safety and stability of the project. In this study, a new governing equation for thermal consolidation of saturated marine sediments is proposed, by considering the depth variability of the marine sediment layer and the time-dependent external loading and temperature. The corresponding one-dimensional (1D) analytical solution for thermal consolidation of saturated marine sediments is derived. The average degree of consolidation (U_a) and the normalized excess pore water pressure (u/u_0) in the saturated marine sediment layer at different depths and time durations are calculated and compared with the typical loading case. The results show that the loading rate of the external force only affects the amplitude of the excess pore water pressure u and does not affect the proportion of u with depth; the depth variability of bulk modulus has a greater effect on the distribution of U_a relative to the depth variability of permeability; the depth variability of permeability has a greater effect on the distribution of u/u_0 with depth relative to the depth variability of bulk modulus when $U_a = 50\%$; the assumption of instant thermal loading will lead to an over-assessment of U_a and u/u_0 . This study provides useful insights for energy geotechnical engineering design and practice.

1. Introduction

When analyzing the long-term safety and stability of geotechnical engineering, such as land reclamation, embankments, pipelines, mat foundations and spudcan footings, the consolidation of soil layers is one important issue that needs to be seriously concerned, especially for the saturated clay with high compressibility and low permeability, e.g., marine soils (Zhu et al., 2018; Feng et al., 2019, 2021; Indraratna et al., 2016; Zhao et al., 2021; Zhang et al., 2021; Yi et al., 2021; Cui et al., 2022; Cui et al., 2023). In recent years, with the rapid economic development, geotechnical infrastructures have expanded their domain into the field of energy geotechnics (McCartney et al., 2019), such as energy piles, geothermal extraction, geological waste disposal, and submarine high-temperature oil and gas pipelines, as shown in Fig. 1 (Gashti et al., 2014; Norris, 2017; Cheng et al., 2020). Especially for submarine pipelines, with the growing exploitation of oil and gas into deep and even ultra-deep water, submarine pipelines are usually laid directly on soft marine sediments with low permeability. During the

transporting of high-temperature oil and gas in pipelines, the out-wall temperature of pipelines can also reach 20 °C–50 °C despite the temperature insulation measures (Bai and Niedzwecki, 2014), causing temperature changes in the sediments, which affect the physical and mechanical properties of the sediments (Zhang et al., 2022). Neglecting the effect of temperature on evaluating the response of buried pipelines can possibly lead to misunderstandings regarding the structural behavior of buried pipelines, the geotechnical response of the seabed, and seabed–pipeline interaction (Shahrokhbadi et al., 2020).

Normally, the consolidation of marine sediments around pipelines would occur both during the laying of pipelines (by external loading, such as the upper pipeline weight) and the transport of high-temperature oil and gas in pipelines (by heating). During the dissipation of excess pore water pressure, the vertical penetration and horizontal breakout resistance of pipelines would change markedly (Krost et al., 2011; Chatterjee et al., 2013), which directly influences the axial pipe–soil resistance and affects many aspects of pipeline design, such as stability on slopes, geohazard vulnerability, lateral buckling, and pipe

* Corresponding author. Department of Ocean Science and Engineering, Southern University of Science and Technology, Shenzhen, China.

E-mail addresses: humj2021@connect.hku.hk (M.-J. Hu), fengwq@sustech.edu.cn (W.-Q. Feng), junyang@hku.hk (J. Yang).

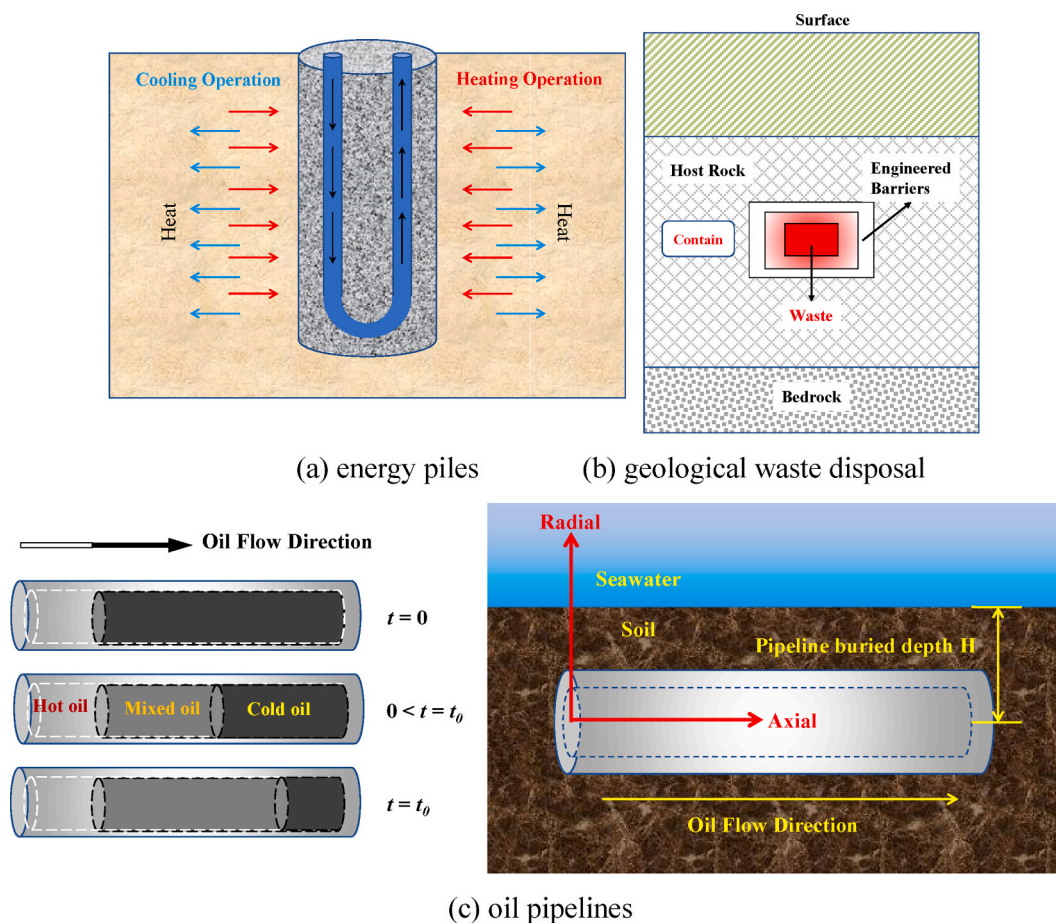


Fig. 1. Typical examples of energy geotechnics.

walking behavior (Shi et al., 2019; Liu et al., 2021; Jin et al., 2021; Jiang and Dong, 2022). Therefore, it is of great importance to study the thermal consolidation of saturated marine sediments under time-dependent loading.

The thermal consolidation of sediments has been studied by many scholars. Paaswell (1967) firstly introduced the concept of thermal consolidation when he found heating test results of soils are very similar to those of standard oedometer tests. Delage et al. (2000) presented an experimental study of Boom clay on the thermal volume change, the thermal consolidation, and the temperature effects on permeability. Liu et al. (2019) proposed a one-dimensional analytical solution for the thermal consolidation of marine clay by considering the effect of viscosity. Wang et al. (2022) conducted two series of temperature-controlled model tests and found that the pipeline with high temperature (55 °C) exhibits 20% larger initial axial soil resistance stiffness than the low-temperature pipeline (15 °C). The results show that the thermal consolidation has increased the soil stiffness around the high-temperature pipeline. Yang et al. (2022) conducted thermal consolidation tests of saturated silty clay under different temperature paths and confining pressures.

However, all the thermal consolidation studies mentioned above did not consider the effect of the external loading or just assumed that the external loading is applied instantly. In fact, the external loading from construction and operation normally takes some time (Zhu and Yin, 1999; Xu et al., 2018). Hanna et al. (2013) found that Terzaghi's approximation of taking the ramp load as instantaneous load overestimates the degree of consolidation by approximately 10%. Wu et al. (2009) derived an analytical solution for 1D thermal consolidation of single drained saturated soils considering time-dependent loading. However, it was assumed that the thermal loading and the external

loading are applied at the same time, which is only one special case in practice. Normally, the sediments under the energy geotechnics, such as submarine high-temperature oil and gas pipelines, would be applied the external loading first during the construction period and be applied the thermal loading during the operation period.

Apart from that, the thermal consolidation theories used above are not rigorous, because they did not consider the variation of permeability and compressibility of marine sediment layers in the vertical direction. Field and laboratory tests on marine sediments have shown that the permeability and compressibility of clay are generally not constant (Ward et al., 1959, 1965; Cui et al., 2018; Feng and Yin, 2020). Therefore, some scholars have attempted to consider the effects of depth variability of sediments in their studies (Schiffman and Gibson, 1964; Poskitt, 1969; Mahmoud and Deresiewicz, 1980; Zhu and Yin, 1999, 2012; Abbasi et al., 2007). For example, recently, Xu et al. (2018) proposed a 1D consolidation solution by considering depth-dependent parameters of the sediment layer, which is subjected to complicated time-dependent loadings at the ground surface; Li et al. (2020) investigated the consolidation responses of rheological aquitards to tide-induced groundwater fluctuations in coastal soft deposits by considering the depth-dependent properties of the initial permeability and compressibility.

In this study, efforts are made to bridge the research gap mentioned above by proposing an analytical solution to the thermal consolidation of a saturated sediment layer considering depth variability and time-dependent loading. Based on the new analytical solution, a systematic study is performed on the effects of depth variability parameters and on the effects of beginning time and duration of the load. This study has a great practical relevance to the design and practice of energy geotechnical engineering.

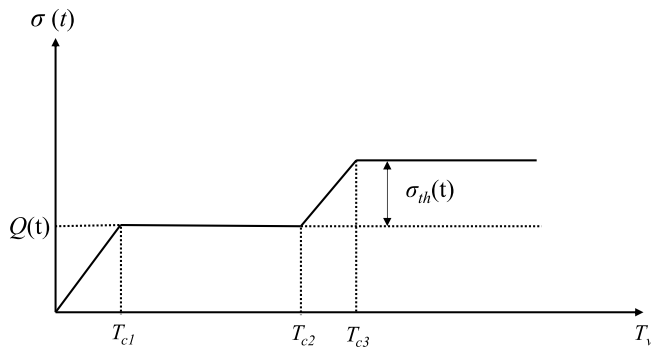


Fig. 2. Schematic drawing of time-dependent non-thermal loading and thermal loading.

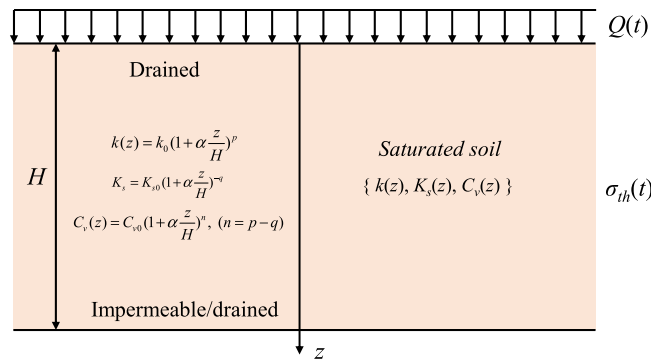


Fig. 3. Schematic drawing of 1D thermal consolidation model for a saturated sediment layer.

Table 1
Values of the parameters in the calculation.

H (m)	N	T _T (°C)	q _c (kPa)	m ₀ (kPa ⁻¹)
10	0.0004	75	200	0.000157
K ₀	T _{c1}	T _{c2}	T _{c3}	
0.7	0.1	0.2	0.3	

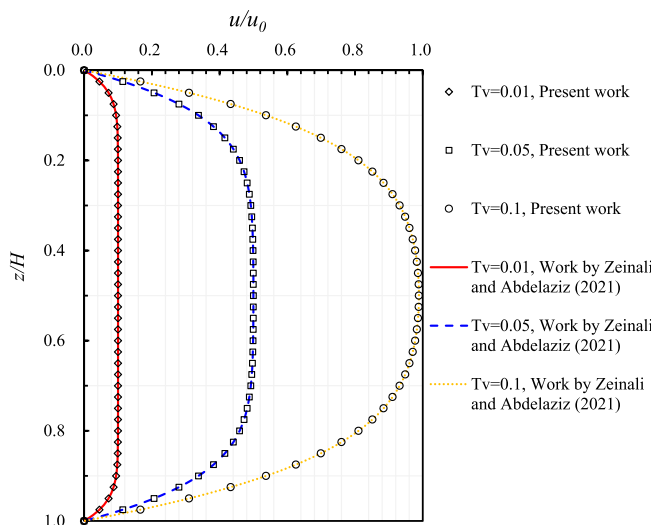


Fig. 4. Comparison of excess pore water pressure distribution at different time factors between solution of Zeinali and Abdelaziz (2021) and present solution.

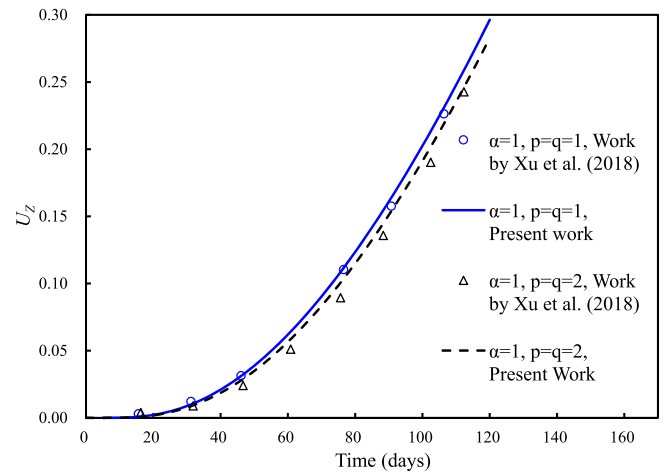


Fig. 5. Comparison of consolidation degree at a certain depth ($z/H = 0.375$) between solution of Xu et al. (2018) and present solution.

2. The governing equation and analytical solution

2.1. The assumptions of thermal consolidation

In order to derive the thermal consolidation in 1D condition, the assumptions are expressed as follows:

- (1) The soil is fully saturated.
- (2) The soil particles and water are incompressible.
- (3) The external loading only produces unidirectional seepage and compression.
- (4) Darcy's law is valid.
- (5) The deformation is caused exclusively by the dissipation of excess pore water pressure.
- (6) The coefficient of thermal expansion of soil particles and water are constant.
- (7) The temperature changes are consistent at all points of the sediment layer.

2.2. The derivation process

When a certain temperature is transferred to the saturated marine sediment, this can lead to a change of pore water pressure, which is referred to as the thermal pore water pressure (u_{th}). The volumetric strain developed from the dissipation of thermal excess pore water pressure is referred as the thermal volume strain (ϵ_{th}). Under the fully drained condition, when the dissipation rate of pore water pressure exceeds the rate of generation of pore water pressure due to thermal formation, no thermal pore water pressure is generated at this time. The thermal volumetric strain is defined as fully drained thermal volume strain ($\epsilon_{th,fully\ drained}$). On the other hand, if a certain temperature change is applied under the fully undrained conditions, the maximum pore water pressure that can be generated is called fully undrained thermal pore water pressure ($u_{th,fully\ undrained}$). Zeinali and Abdelaziz (2021) proposed a relationship between $u_{th,fully\ undrained}$ and $\epsilon_{th,fully\ drained}$ with the bulk modulus of elasticity (K_s) of the sediment. However, that relationship cannot be used to describe the thermal expansion, which is usually found for over-consolidated sediments (Cekerevac and Laloui, 2004; McCartney et al., 2019). Normally, the heating of normal consolidated soil will cause thermal contraction, while the heating of over-consolidated soil is prone to thermal expansion (Yang et al., 2022). Since the submarine environment is complex, marine sediments often exhibit a wide variation in consolidation ratios. Therefore, it would be more practical if the study could properly describe the thermal consolidation development of sediments with different consolidation ratios. In

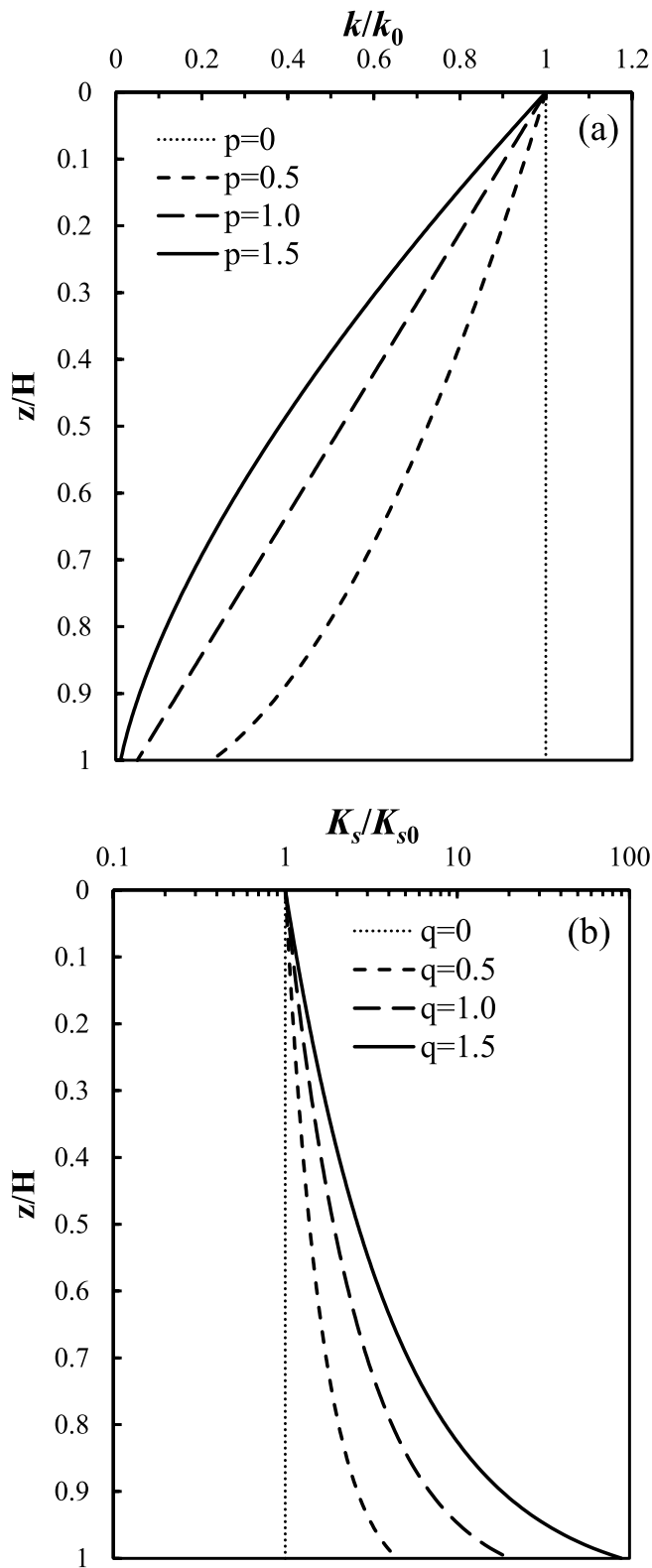


Fig. 6. The depth-dependent variable distributions: (a) normalized permeability and (b) normalized bulk modulus.

this study, a new relationship that can consider both thermal expansion and thermal contraction is proposed and expressed as follows:

$$u_{th,fully\ undrained} = K_s \varepsilon_{th,fully\ drained} = K_s \Delta T [(n_0 - n_{th})(\alpha_s - \alpha_w) + \alpha_{st}] \quad (1)$$

where n_0 is porosity of the marine sediment; n_{th} represents equilibrium porosity of the marine sediment subjected to the temperature variation;

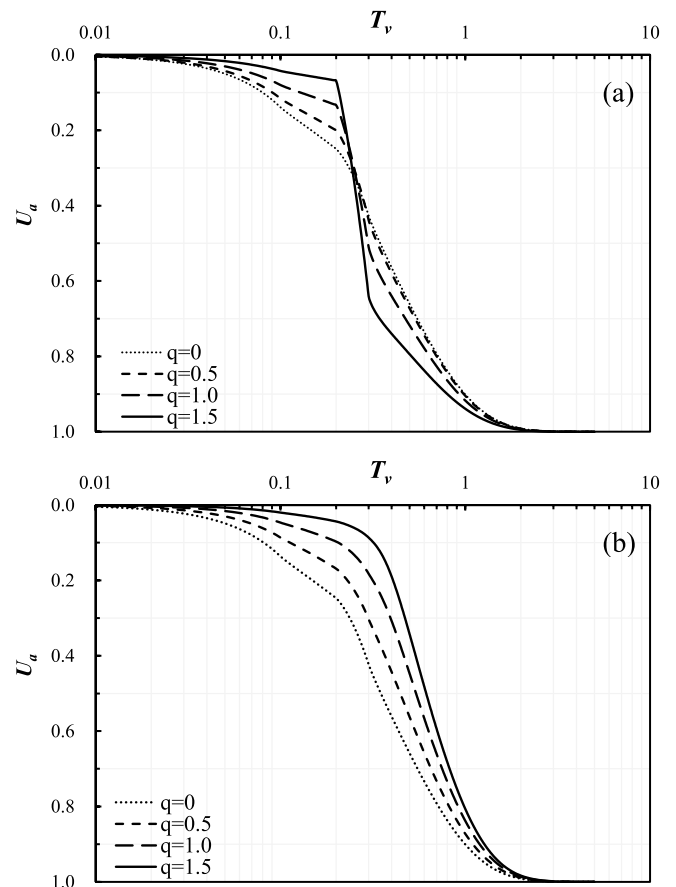


Fig. 7. Average degree of thermal consolidation for depth-dependent bulk modulus with constant permeability: (a) double drainage and (b) single drainage.

ΔT denotes the temperature change; $\alpha_s, \alpha_w, \alpha_{st}$ are volumetric thermal expansion coefficients of soil particles, pore water, and soil fabric, respectively. When n_{th} is larger than n_0 , the thermal expansion of over-consolidated marine sediments can be considered. In comparison, the thermal contraction of the marine sediment can be achieved when n_{th} is smaller than n_0 . Specially, when n_{th} equals 0, Eq. (1) can be degraded to that in Zeinali and Abdelaziz (2021). Let $N = [(n_0 - n_{th})(\alpha_s - \alpha_w) + \alpha_{st}]$, Eq. (1) can be rewritten as Eq. (2):

$$u_{th,fully\ undrained} = K_s \Delta TN \quad (2)$$

In practice, the dissipation of thermal pore water pressure is between the fully drained and fully undrained. Therefore, the relationship between thermal pore water pressure (u_{th}) and thermal volumetric strain (ε_{th}) can be shown as:

$$u_{th} = K_s (\varepsilon_{th,fully\ drained} - \varepsilon_{th}) = K_s \Delta TN - K_s \varepsilon_{th} \quad (3)$$

When only the effect of temperature is considered, the stress in the sediment is expressed according to the effective stress principle as:

$$\sigma_{th} = \sigma_{th}' + u_{th} \quad (4)$$

where σ_{th}' and σ_{th} are the effective stress and total stress in the sediment due to the thermal loading, respectively.

Combining Eqs. (3) and (4), it can lead to:

$$\sigma_{th} = K_s \Delta TN \quad (5)$$

Considering both the thermal loading and time-dependent loading, the total loading can be expressed as:

$$\sigma(t) = Q(t) + \sigma_{th}(t) \quad (6)$$

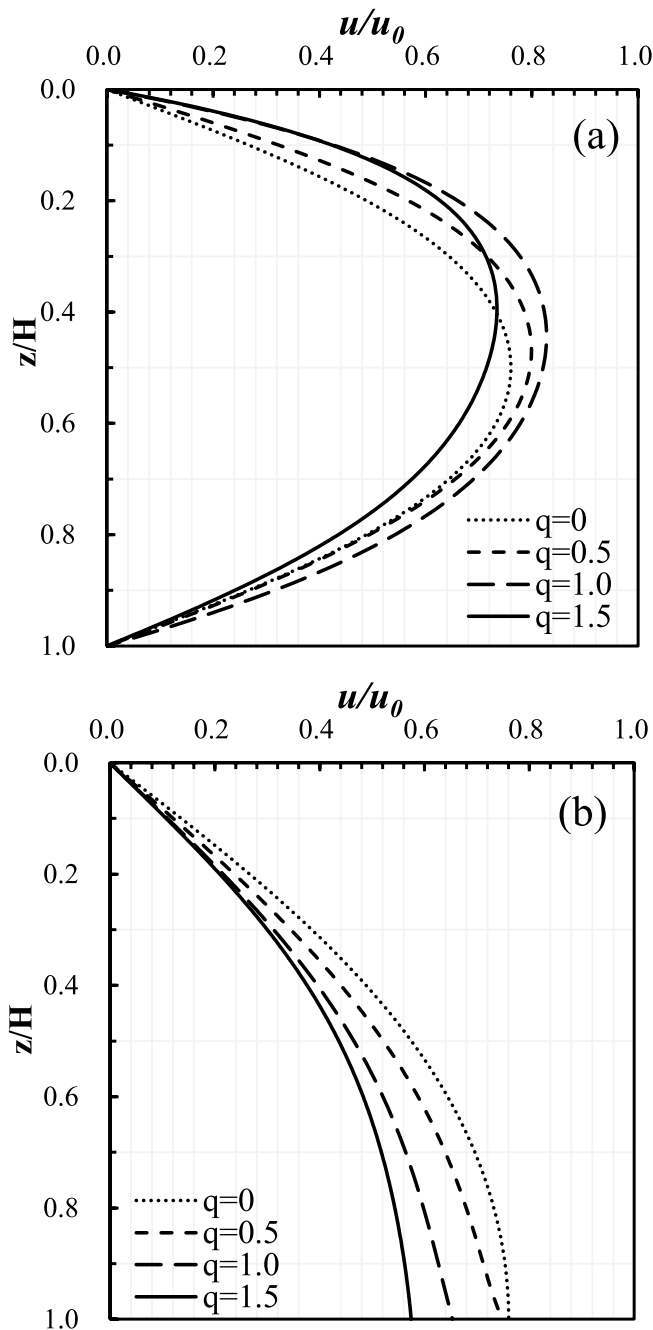


Fig. 8. Excess pore water pressure of 50% average degree for depth-dependent bulk modulus with constant permeability: (a) double drainage and (b) single drainage.

where $\sigma(t)$ and $Q(t)$ are the total loading and the time-dependent non-thermal loading in the sediment, respectively, as shown in Fig. 2.

The governing equation for the thermal consolidation of the saturated marine sediments considering depth variability under time-dependent loading is given by:

$$\frac{\partial^2 u}{\partial z^2} + \frac{1}{k} \frac{dk}{dz} \frac{\partial u}{\partial z} = \frac{1}{C_v(z)} \left(\frac{\partial u}{\partial t} - \frac{\partial \sigma(t)}{\partial t} \right) \quad (7)$$

$$k(z) = k_0 \left(1 + \alpha \frac{z}{H} \right)^p \quad (8)$$

$$m_v(z) = m_0 \left(1 + \alpha \frac{z}{H} \right)^q \quad (9)$$

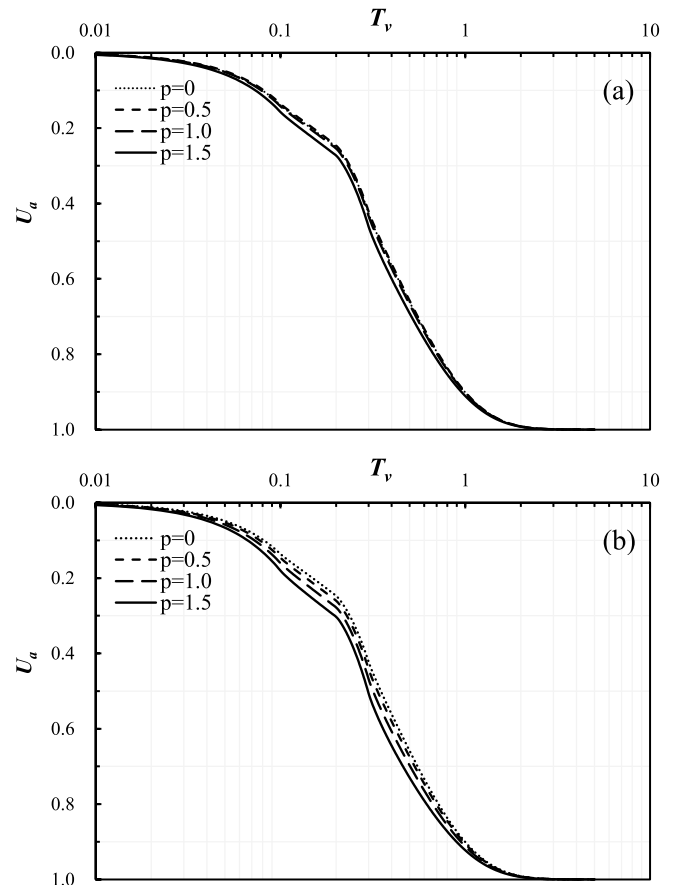


Fig. 9. Average degree of thermal consolidation for depth-dependent permeability with constant bulk modulus: (a) double drainage and (b) single drainage.

$$K_s = \frac{1 + 2K_0}{3} \frac{1}{m_v} = K_{s0} \left(1 + \alpha \frac{z}{H} \right)^{-q} \quad (10)$$

$$C_v(z) = \frac{k(z)}{\gamma_w m_v(z)} = C_0 \left(1 + \alpha \frac{z}{H} \right)^n, \quad \left(n = p - q; C_0 = \frac{k_0}{m_0 \gamma_w} \right) \quad (11)$$

where u is the excess pore water pressure of the sediment layer; t denotes the duration of consolidation; C_v represents the coefficient of consolidation of the sediment layer; γ_w is the unit weight of water; K_0 is the lateral coefficient of earth pressure; and $p, q, n, \alpha, k_0, m_0, K_{s0}$ and C_0 are constants, as shown in Fig. 3.

For the governing Eq. (7), the following two typical boundary conditions are considered:

$$\begin{cases} u(0, t) = 0 \\ \left. \frac{\partial u}{\partial z} \right|_{z=H} = 0 \end{cases} \quad (12)$$

$$\begin{cases} u(0, t) = 0 \\ u(H, t) = 0 \end{cases} \quad (13)$$

Eq. (12) expresses that the top of the layer is drained and the bottom of the layer is undrained (i.e., single-drained condition). Eq. (13) expresses that both the top and bottom of the layer are drained (i.e., double-drained condition).

Eq. (7) is a non-homogeneous partial differential equation and it can be simplified as a superposition of a homogeneous equation and a non-homogeneous equation with different initial conditions. First, the homogeneous equation is expressed as:

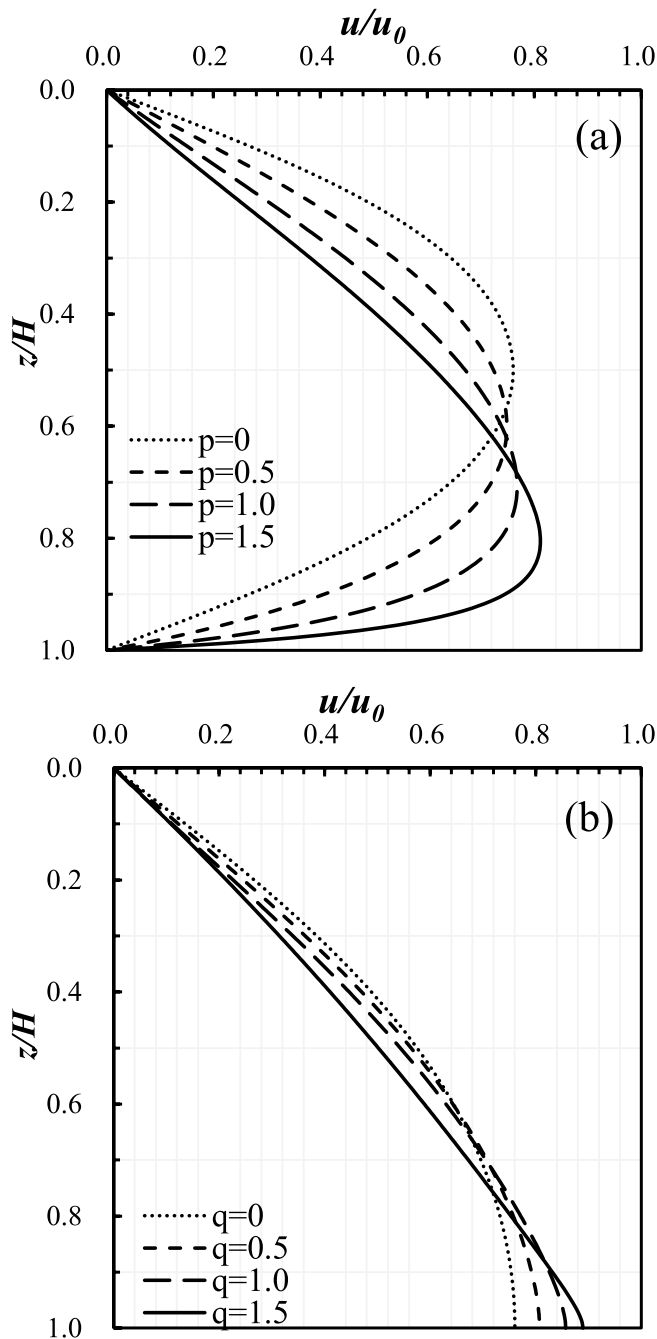


Fig. 10. Excess pore water pressure of 50% average degree for depth-dependent permeability with constant bulk modulus: (a) double drainage and (b) single drainage.

$$\frac{\partial u}{\partial t} = C_v(z) \left(\frac{\partial^2 u}{\partial z^2} + \frac{1}{k} \frac{dk}{dz} \frac{\partial u}{\partial z} \right) \quad (14)$$

According to Duhamel's principle (Özsisik, 1980), Eq. (7) can be solved from the homogeneous equation of Eq. (14). Eq. (14) can be solved by the separation of variables method. Zhu and Yin (2012) solved this type of homogeneous cases and obtained the analytical solution.

When $n \neq 2$ and $\alpha \neq 0$, the following relationships are obtained (Schiffman and Gibson, 1964):

$$y = \left(1 + \alpha \frac{z}{H} \right)^{1-\frac{n}{2}} \quad (15)$$

$$u(z, t) = u(y, t) = y^{\frac{1-p}{2-n}} w(y, t) \quad (16)$$

By substituting Eqs. (15) and (16) into Eq. (14), Eq. (14) can be rewritten as:

$$\frac{\partial^2 w}{\partial y^2} + \frac{1}{y} \frac{\partial w}{\partial y} - \frac{v^2}{y^2} w = \frac{4H^2}{\alpha^2(2-n)^2 C_0} \frac{\partial w}{\partial t} \quad (17)$$

where $v = |(1-p)/(2-n)|$. Using the separation of variables method, Eq. (17) can be solved with the boundary conditions of Eqs. (12) and (13). The analytical solution is obtained as:

$$u = u_0 y^B \sum_{m=1}^{+\infty} C_m Z_v^m(y) \left(e^{-\frac{\pi^2 \eta_m^2}{4\alpha^2} T_v} \right) \quad (18)$$

$$T_v(t) = \frac{\alpha^2(2-n)^2 c_v \eta_1^2 t}{\pi^2 H^2} \quad (19)$$

$$C_m = \frac{\int_1^b y^{\frac{1}{2}} Z_v^m(y) dy}{\int_1^b y [Z_v^m(y)]^2 dy} \quad (20)$$

$$b = (1 + \alpha)^{1-\frac{n}{2}} \quad (21)$$

$$Z_\mu^m(x) = Y_\nu(\eta_m) J_\mu(\eta_m x) - J_\nu(\eta_m) Y_\mu(\eta_m x) \quad (22)$$

where $B=(1-p)/(2-n)$; u_0 denotes the initial excess pore-water pressure (usually zero in the ramp loading); T_v is the time factor; C_m and b are calculation parameters; J_ν, Y_ν are Bessel functions of the first and second kind of order ν , respectively; J_μ, Y_μ are Bessel functions of the first and second kind of order μ , respectively; and η_m are eigenvalues arranged in increasing order ($m = 1, 2, 3, \dots, \infty$).

For the double-drained boundary, η_m are the positive roots of the following equation for variable η :

$$R(\eta) = Z_\nu(b) = Y_\nu(\eta) J_\nu(\eta b) - J_\nu(\eta) Y_\nu(\eta b) = 0 \quad (23)$$

The constant C_m for the double-drained boundary is:

$$C_m = \begin{cases} \frac{2\pi[2 + \pi\eta_m b^{1-\nu} Z_{\nu-1}^m(b)]^2}{4 - [b\pi\eta_m Z_{\nu+1}^m(b)]^2}, \nu = \frac{1-p}{2-n} \\ \frac{2\pi[2 - \pi\eta_m b^{1+\nu} Z_{\nu+1}^m(b)]^2}{4 - [b\pi\eta_m Z_{\nu+1}^m(b)]^2}, \nu = \frac{p-1}{2-n} \end{cases} \quad (24)$$

Similarly, for the single-drained boundary, η_m are the positive roots of the following equation for variable η :

$$R(\eta) = \frac{1-p}{2-n} Z_\nu(b) + b Z_\nu'(b) = 0 \quad (25)$$

The constant C_m for the single-drained boundary is:

$$C_m = \frac{4\pi}{4 - [b\pi\eta_m Z_{\nu+1}^m(b)]^2} \quad (26)$$

In this study, the time loading pattern of the time-dependent loading in construction period is different from that of the thermal loading in operation period, the expressions are expressed as follow:

$$Q(t) = \begin{cases} Q_c \frac{t}{t_{c1}}, 0 \leq t < t_{c1} \\ Q_c, t \geq t_{c1} \end{cases} \quad (27)$$

$$T(t) = \begin{cases} 0, 0 \leq t < t_{c2} \\ T_T \frac{(t - t_{c2})}{(t_{c3} - t_{c2})}, t_{c2} \leq t < t_{c3} \\ T_T, t \geq t_{c3} \end{cases} \quad (28)$$

$$T_{c1} = T_v(t_{c1}), T_{c2} = T_v(t_{c2}), T_{c3} = T_v(t_{c3}) \quad (29)$$

where t_{c1}, t_{c2}, t_{c3} are the turning point in time for loading; T_{c1}, T_{c2}, T_{c3}

are the corresponding time factor of t_{c1} , t_{c2} , t_{c3} , respectively; Q_c and T_T are the final applied loading and the final temperature. Since we assume that the initial temperature is zero, then $T_T = \Delta T$.

Based on Duhamel's principle and Eq. (14), Eq. (7) can be solved and the solution is shown as:

$$u = \begin{cases} \frac{Q_c}{T_{c1}} \frac{4\eta_1^2 y^B}{\pi^2} \sum_{m=1}^{+\infty} C_m Z_v^m(y) \frac{1}{\eta_m^2} \left(1 - e^{-\frac{\pi^2 \eta_m^2 T_v}{4\eta_1^2}} \right), 0 \leq T_v \leq T_{c1} \\ \frac{Q_c}{T_{c1}} \frac{4\eta_1^2 y^B}{\pi^2} \sum_{m=1}^{+\infty} C_m Z_v^m(y) \frac{1}{\eta_m^2} \left[e^{-\frac{\pi^2 \eta_m^2 (T_v - T_{c1})}{4\eta_1^2}} - e^{-\frac{\pi^2 \eta_m^2 T_v}{4\eta_1^2}} \right], T_{c1} < T_v \leq T_{c2} \\ \frac{Q_c}{T_{c1}} \frac{4\eta_1^2 y^B}{\pi^2} \sum_{m=1}^{+\infty} C_m Z_v^m(y) \frac{1}{\eta_m^2} \left[e^{-\frac{\pi^2 \eta_m^2 (T_v - T_{c1})}{4\eta_1^2}} - e^{-\frac{\pi^2 \eta_m^2 T_v}{4\eta_1^2}} \right] + \\ \left(K_s N T_T \frac{1}{T_{c3} - T_{c2}} \right) \frac{4\eta_1^2 y^B}{\pi^2} \sum_{m=1}^{+\infty} C_m Z_v^m(y) \frac{1}{\eta_m^2} \left[1 - e^{-\frac{\pi^2 \eta_m^2 (T_v - T_{c2})}{4\eta_1^2}} \right], T_{c2} < T_v \leq T_{c3} \\ \frac{Q_c}{T_{c1}} \frac{4\eta_1^2 y^B}{\pi^2} \sum_{m=1}^{+\infty} C_m Z_v^m(y) \frac{1}{\eta_m^2} \left[e^{-\frac{\pi^2 \eta_m^2 (T_v - T_{c1})}{4\eta_1^2}} - e^{-\frac{\pi^2 \eta_m^2 T_v}{4\eta_1^2}} \right] + \\ \left(K_s N T_T \frac{1}{T_{c3} - T_{c2}} \right) \frac{4\eta_1^2 y^B}{\pi^2} \sum_{m=1}^{+\infty} C_m Z_v^m(y) \frac{1}{\eta_m^2} \left[e^{-\frac{\pi^2 \eta_m^2 (T_v - T_{c3})}{4\eta_1^2}} - e^{-\frac{\pi^2 \eta_m^2 (T_v - T_{c2})}{4\eta_1^2}} \right], T_{c3} < T_v \end{cases} \quad (30)$$

The average degree of consolidation U_a is defined as:

$$U_a(t) = \frac{\int_0^H \sigma(t) - u(z, t) dz}{\int_0^H \sigma(t = \infty) dz} \quad (31)$$

It is worth noting that this study is concerned with the inadequacy of the current research presented and has made simplifying assumptions about some parameters, resulting in inconsistencies with reality, such as assuming constant coefficients of thermal expansion for soil particles and water. Many researchers considered these parameter variations to be

small; however, a more rigorous and realistic study would be of great value.

$$U_a(t) = \begin{cases} \frac{\int_0^H \left\{ Q_c \left[\frac{T_v}{T_{c1}} - \frac{1}{T_{c1}} \frac{4\eta_1^2 y^B}{\pi^2} \sum_{m=1}^{+\infty} C_m Z_v^m(y) \frac{1}{\eta_m^2} \left(1 - e^{-\frac{\pi^2 \eta_m^2 T_v}{4\eta_1^2}} \right) \right] \right\} dz}{\int_0^H (K_s N T_T + Q_c) dz}, 0 \leq T_v \leq T_{c1} \\ \frac{\int_0^H \left\{ Q_c \left[1 - \frac{1}{T_{c1}} \frac{4\eta_1^2 y^B}{\pi^2} \sum_{m=1}^{+\infty} C_m Z_v^m(y) \frac{1}{\eta_m^2} \left(e^{-\frac{\pi^2 \eta_m^2 (T_v - T_{c1})}{4\eta_1^2}} - e^{-\frac{\pi^2 \eta_m^2 T_v}{4\eta_1^2}} \right) \right] \right\} dz}{\int_0^H (K_s N T_T + Q_c) dz}, T_{c1} < T_v \leq T_{c2} \\ \frac{\int_0^H \left\{ Q_c \left[1 - \frac{1}{T_{c1}} \frac{4\eta_1^2 y^B}{\pi^2} \sum_{m=1}^{+\infty} C_m Z_v^m(y) \frac{1}{\eta_m^2} \left(e^{-\frac{\pi^2 \eta_m^2 (T_v - T_{c1})}{4\eta_1^2}} - e^{-\frac{\pi^2 \eta_m^2 T_v}{4\eta_1^2}} \right) \right] + \left[\frac{K_s N T_T}{T_{c3} - T_{c2}} \left[T_v - T_{c2} - \frac{4\eta_1^2 y^B}{\pi^2} \sum_{m=1}^{+\infty} C_m Z_v^m(y) \frac{1}{\eta_m^2} \left(1 - e^{-\frac{\pi^2 \eta_m^2 (T_v - T_{c2})}{4\eta_1^2}} \right) \right] \right] \right\} dz}{\int_0^H (K_s N T_T + Q_c) dz}, T_{c2} < T_v \leq T_{c3} \\ \frac{\int_0^H \left\{ Q_c \left[1 - \frac{1}{T_{c1}} \frac{4\eta_1^2 y^B}{\pi^2} \sum_{m=1}^{+\infty} C_m Z_v^m(y) \frac{1}{\eta_m^2} \left(e^{-\frac{\pi^2 \eta_m^2 (T_v - T_{c1})}{4\eta_1^2}} - e^{-\frac{\pi^2 \eta_m^2 T_v}{4\eta_1^2}} \right) \right] + \frac{K_s N T_T}{T_{c3} - T_{c2}} \left[T_{c3} - T_{c2} - \frac{4\eta_1^2 y^B}{\pi^2} \sum_{m=1}^{+\infty} C_m Z_v^m(y) \frac{1}{\eta_m^2} \left(e^{-\frac{\pi^2 \eta_m^2 (T_v - T_{c3})}{4\eta_1^2}} - e^{-\frac{\pi^2 \eta_m^2 (T_v - T_{c2})}{4\eta_1^2}} \right) \right] \right\} dz}{\int_0^H (K_s N T_T + Q_c) dz}, T_{c3} < T_v \end{cases} \quad (32)$$

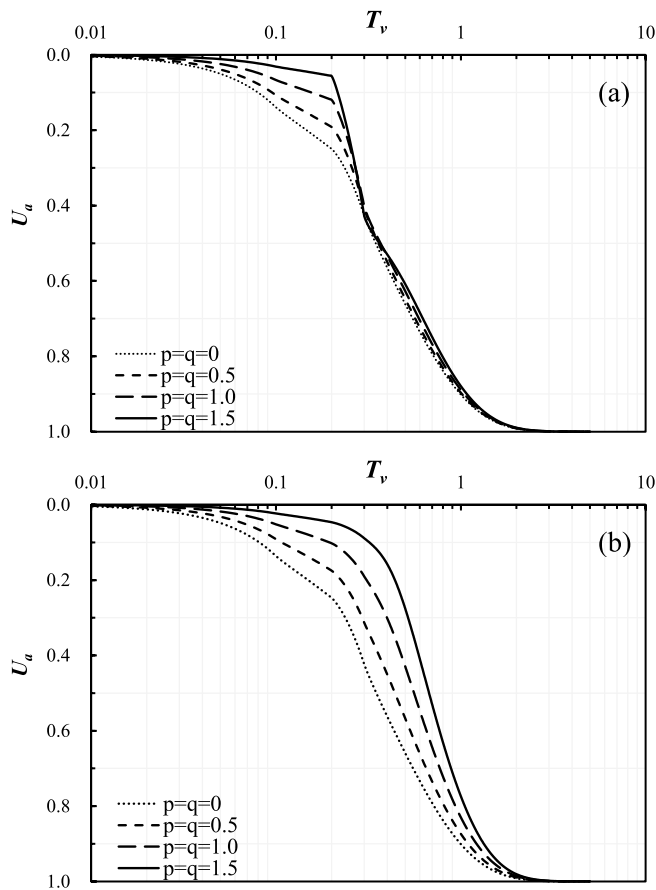


Fig. 11. Average degree of thermal consolidation for constant C_v : (a) double drainage and (b) single drainage.

3. Special cases

Based on Zeinali and Abdelaziz (2021), the parameters used in this study are listed in Table 1. According to Eq. (30), the value of excess pore water pressure u is affected by the thermal parameter N , the temperature change (ΔT or T_T), the loading time, depth-dependent parameters α , p , q and boundary conditions. In order to reduce the interference of these parameters, the normalized excess pore water pressure u/u_0 (Eq. (33)) is defined and used to study the distribution of excess pore water pressure at different periods and depths in the marine sediment layer. In the following part, different cases are set up, programmed, calculated and analyzed by software MATLAB, and the analyzed results are compared with the theoretical solution that does not consider depth variability (i.e. $p = q = 0$).

$$u / u_0 = u / \sigma(t = \infty) = u / (Q_c + K_s N T_T) \quad (33)$$

3.1. Evaluation of the proposed solution

Firstly, when considering the thermal consolidation in a homogeneous sediment layer ($p = q = 0$) and without the loading ($Q_c = 0$), the excess pore water pressures at different time factors under double drainage are calculated. The excess pore water pressure distribution is compared with Zeinali and Abdelaziz (2021), as shown in Fig. 4. It is shown that the results fit well with each other. The excess pore water pressure distribution of a homogeneous sediment layer is symmetrical and the same with the classic Terzaghi's theory. However, under natural conditions, the sediment layer is most likely nonhomogeneous: the deeper the sediment, the denser it is, with smaller permeability coefficient and higher bulk modulus.

Xu et al. (2018) proposed a 1-D consolidation solution by considering

depth-dependent parameters of the sediment layer, which is subjected to complicated time-dependent loadings, such as rectangular and triangular cyclic loading, at the ground surface. For the comparison, the half cycle of the triangular cyclic loading (the monotonic loading) is chosen. Xu et al. (2018) chose a certain depth ($z/H = 0.375$) as the calculated position to analyze the development of consolidation degree with time. The values of constant parameter they used are: $m_0 = 1 \times 10^{-7} \text{ Pa}^{-1}$, $k_0 = 8.64 \times 10^{-6} \text{ m/day}$. The monotonic loading duration is 120 days. Then, using this study's proposed solution and considering the consolidation as an insulated environment ($\Delta T = 0$), the consolidation degree at a certain depth ($z/H = 0.375$) under double drainage is calculated. The results of consolidation degree are compared with Xu et al. (2018), as shown in Fig. 5. The result shows a good agreement. The small deviation may be the influence of different calculation methods and

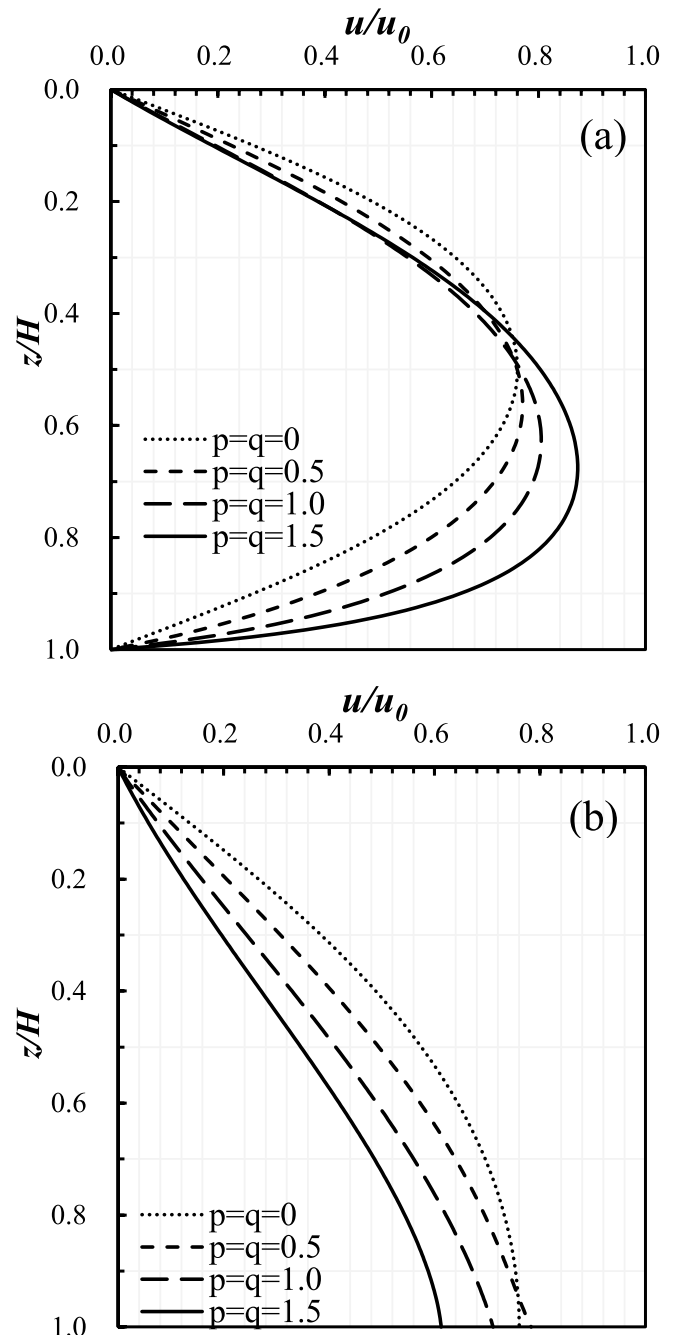


Fig. 12. Excess pore water pressure of 50% average degree for constant C_v : (a) double drainage and (b) single drainage.

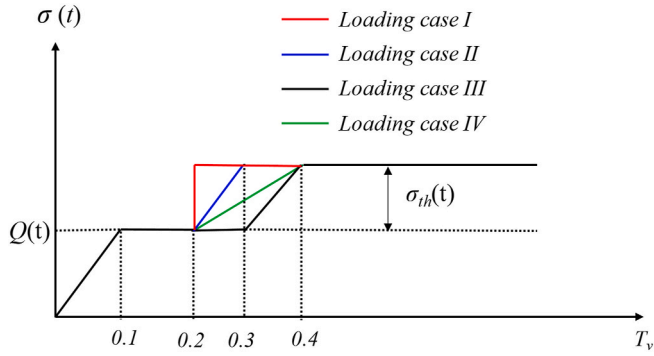


Fig. 13. The different time-dependent loading and heating cases.

calculation accuracy.

As there are no relevant studies on thermal consolidation that consider the depth variability of sediments, the subsequent analysis of some parameters in this study may provide guidance for relevant engineering construction and safety assessments. Fig. 6 represents the distributions of the three depth-dependent parameters under different p and q values, when $\alpha = -0.95$. The value of α is a reasonable assumption and the effect on the value of α is not the concern of this paper. For different values of p and q , Fig. 6 indicates that the permeability of the sediment will decrease with the increase of depth, while the bulk modulus of the sediment will increase, which corresponds to the actual situation. With the increase of the p and q , the variation range of upper and lower parameters of the sediment layer will also increase, especially the variation value of bulk modulus will increase significantly.

3.2. Thermal consolidation cases of depth-dependent bulk modulus with constant permeability

When considering $\alpha = -0.95$ and $p = 0$, it means that the permeability of the sediment layer is constant, while the bulk modulus is depth-dependent. According to Eq. (32), the average degree of consolidation is calculated and analyzed, and the results are compared in Fig. 7.

From Fig. 7, it is seen that, for both double drainage and single drainage conditions, the average degree of consolidation U_a for the sediment layer decreases with the increase of q when T_v is less than T_{c2} . However, when T_v is greater than T_{c2} , the change of U_a under single drainage remains the same pattern with the increase of q , while the change of that under double drainage leads to a reverse one. This phenomenon can be explained by the change of bulk modulus. In this study, the depth-dependent bulk modulus increase as q increases, so does the thermal loading and the resulting u . It can be seen from the expression of Eq. (32) that the proportion of the thermal loading relative to the external force load increases with the increase of q , and that the lower part of the sediment layer would induced a bigger value of u than the upper part. Therefore, with the increase of q , the general dissipation of u and the increase of U_a under double drainage would be faster than that of single drainage. Thus, producing the difference as shown in Fig. 7.

Fig. 8 represents the distributions of the normalized excess pore water pressure u/u_0 of the sediment layer under double drainage and single drainage conditions for $U_a = 50\%$ and $p = 0$. It is seen from Fig. 8 (a) that, when $p = 0$, the location of the maximum value of u/u_0 shifts slightly upwards with the increase of q . When $q = 0$, the location of the maximum value of u/u_0 is the middle of the sediment layer, which is

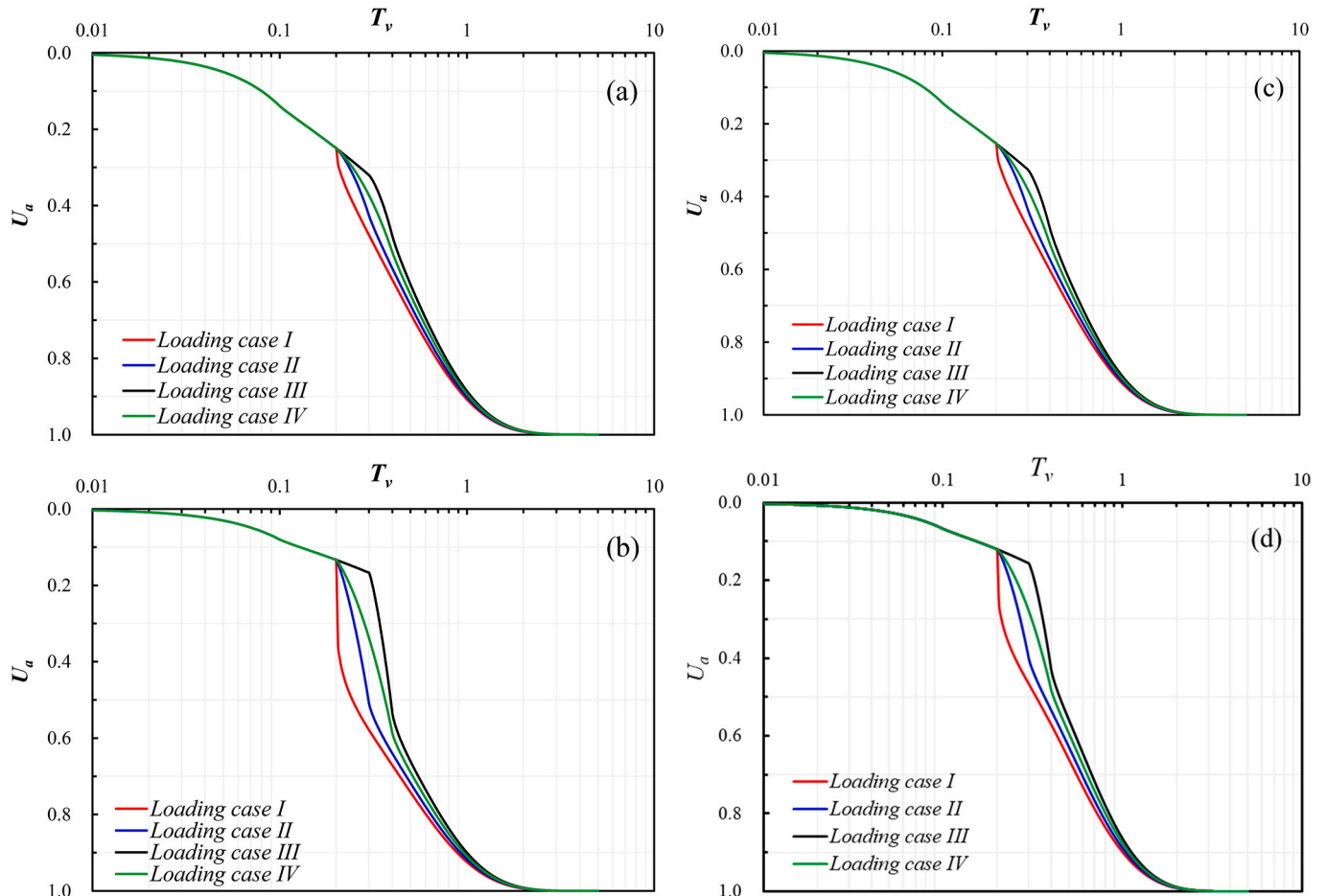


Fig. 14. Average degree of thermal consolidation under double drainage: (a) $p = q = 0$, (b) $p = 0, q = 1$, (c) $p = 1, q = 0$ and (d) $p = q = 1$.

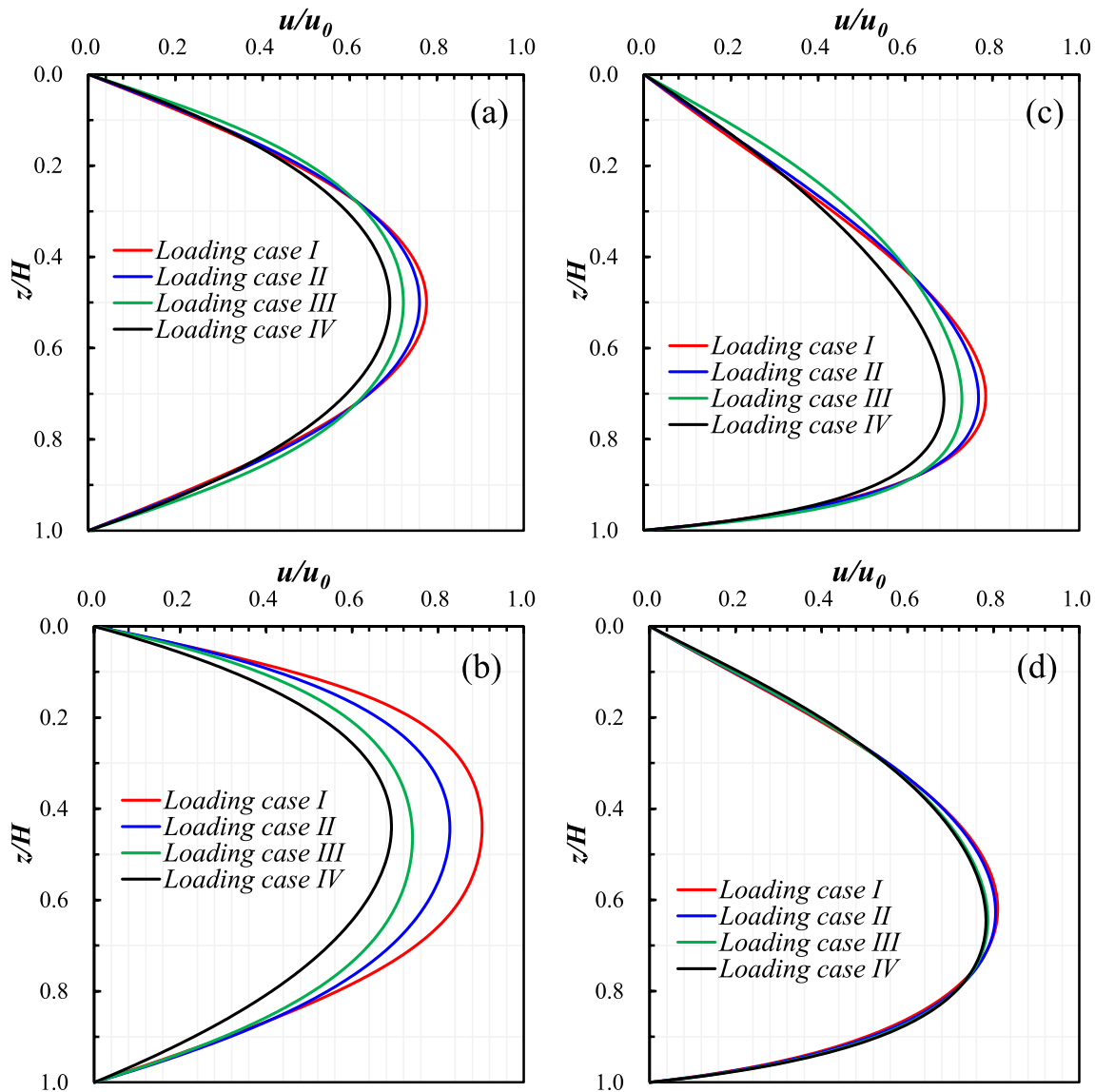


Fig. 15. Excess pore water pressure of 50% average degree under double drainage: (a) $p = q = 0$, (b) $p = 0, q = 1$, (c) $p = 1, q = 0$ and (d) $p = q = 1$.

consistent with the conventional Terzaghi’s consolidation solution. However, the change of the maximum value of u/u_0 with different q does not show a clear trend. From Fig. 8(b), it is shown that the maximum value of u/u_0 under single drainage is always located at the bottom of the sediment layer. Furthermore, for all depths of the sediment layer, the value of u/u_0 decreases with the increase of q , which means that the consolidation solution that does not consider depth variability would give a maximum value of u/u_0 .

3.3. Thermal consolidation cases of depth-dependent permeability with constant bulk modulus

When considering $\alpha = -0.95$ and $q = 0$, it means that the bulk modulus of the sediment layer is constant, while the permeability is depth-dependent. According to Eq. (32), the average degree of consolidation is calculated and analyzed, and the results are compared in Fig. 9.

Fig. 9 shows that, for both double drainage and single drainage conditions, the distribution of U_a of the sediment layer with different p values is very close. With the increase of p , the value of U_a under double drainage is almost the same and the value of U_a under single drainage has less changes compared to that of the case of depth-dependent bulk

modulus with constant permeability.

Fig. 10 represents the distributions of u/u_0 of the sediment layer under both double drainage and single drainage conditions for $U_a = 50\%$ and $q = 0$. It is seen from Fig. 10(a) that, when $q = 0$, the maximum value of u/u_0 under double drainage does not change much with the increase of p , but the location of the maximum value of u/u_0 will move down significantly, from $z/H = 0.5$ ($q = 0$) to $z/H = 0.8$ ($q = 1.5$). From Fig. 10 (b), it is shown that the maximum value of u/u_0 under single drainage is also located at the bottom of the sediment layer. In the upper part of the sediment layer ($z < 0.65H$), the value of u/u_0 at the same depth still decreases with the increase of p . However, at the lower part of the sediment layer ($z > 0.9H$), the value of u/u_0 at the same depth increases as p increases.

3.4. Thermal consolidation cases of depth-dependent permeability and bulk modulus with constant C_v

When considering $\alpha = -0.95$ and $p = q$, it means that the coefficient of consolidation C_v of the sediment layer is constant, while both the permeability and bulk modulus is depth-dependent. According to Eq. (32), the average degree of consolidation is calculated and analyzed, and the results are compared in Fig. 11.

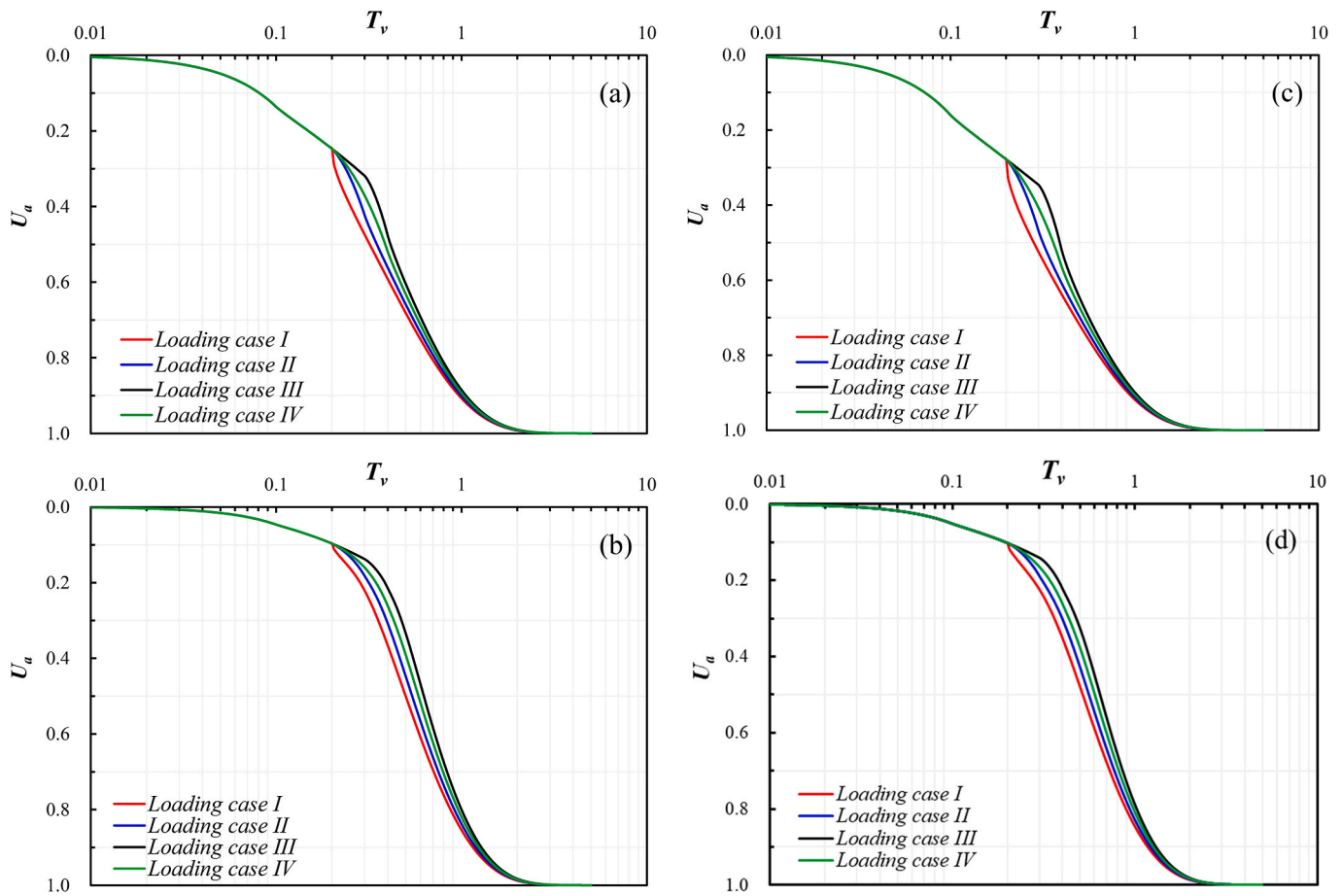


Fig. 16. Average degree of thermal consolidation under single drainage: (a) $p = q = 0$, (b) $p = 0, q = 1$, (c) $p = 1, q = 0$ and (d) $p = q = 1$.

From Fig. 11, it is seen that, for both double drainage and single drainage conditions, the value of U_a of the sediment layer decreases with the increase of q under the same T_v . However, when $T_v = T_{c2}$, the value of U_a under double drainage would follow a much sharp decrease than that of under single drainage.

Fig. 12 represents the distributions of the normalized excess pore water pressure u/u_0 of the sediment layer under both double drainage and single drainage conditions for $U_a = 50\%$ and $p = q$. It is seen from Fig. 12(a) that, when $p = q$, the maximum value of u/u_0 under double drainage would increase with the increase of p ; the location of the maximum value of u/u_0 also shows a tendency to move upwards, but not as significantly as that of the case of depth-dependent permeability with constant bulk modulus. From Fig. 12(b), it is shown that the maximum value of u/u_0 under single drainage is also located at the bottom of the sediment layer. Additionally, Fig. 12(b) shows that the value of u/u_0 decreases with the increase of q , which is true at almost all depths, except the bottom of the sediment layer, where the value of u/u_0 of $q = 0$ is slightly less than that of $q = 0.5$.

4. Influence of thermal loading time

In actual pipeline projects, marine sediments often go through different loading phases. As proposed by Shahrokhbadi et al. (2020), the response of the saturated marine sediments supporting the pipeline can be divided into three phases: post-installation, operation conditions, and the shut-down period. Due to the low permeability of marine sediments, the dissipation of excess pore water pressure by the installation will continue during operation. In terms of operation, it is economically favorable to start the operation as early as possible and keep the heating time as short as possible, as time costs can be reduced. However, from

the perspective of safety, delaying the operation time allows sufficient time for the excess pore water pressure generated by construction (the external force loading) in the sediment layer to dissipate, and the sediment deformation rate is smaller and more stable. What's more, prolonging the heating time can also reduce the excess pore water pressure caused by the thermal loading. It is clear that there is a conflict between these two views. Therefore, it is of practical importance to reasonably determine the time when the pipe starts heating and the duration of heating under the premise of safety.

In this study, there are four loading cases that have been investigated, of which loading case I considers the instant thermal loading, loading case II ($T_{c1} = 0.1, T_{c2} = 0.2, T_{c3} = 0.3$) is the benchmark, loading case III ($T_{c1} = 0.1, T_{c2} = 0.3, T_{c3} = 0.4$) considers delaying the heating time and loading case IV ($T_{c1} = 0.1, T_{c2} = 0.2, T_{c3} = 0.4$) considers prolonging the thermal loading time, as shown in Fig. 13.

In the third part of this study, loading case II in detail under three different special conditions (constant permeability, constant bulk modulus and constant C_v) have been analyzed. In the following study, the analysis of different loading cases under these special conditions will also be carried out in terms of double drainage and single drainage.

4.1. Influence of different loading cases under double drainage

Fig. 14 represents the changes of average degree of thermal consolidation under double drainage for different loading cases. The loading time of external force (q_c) would not change in these loading cases ($T_{c1} = 0.1$). Therefore, we mainly focus on the analysis of the influence of the thermal loading time.

From Fig. 14(a), it can be noticed that under the same T_v , when T_v is greater than T_{c2} , the average degree of consolidation U_a of loading case I

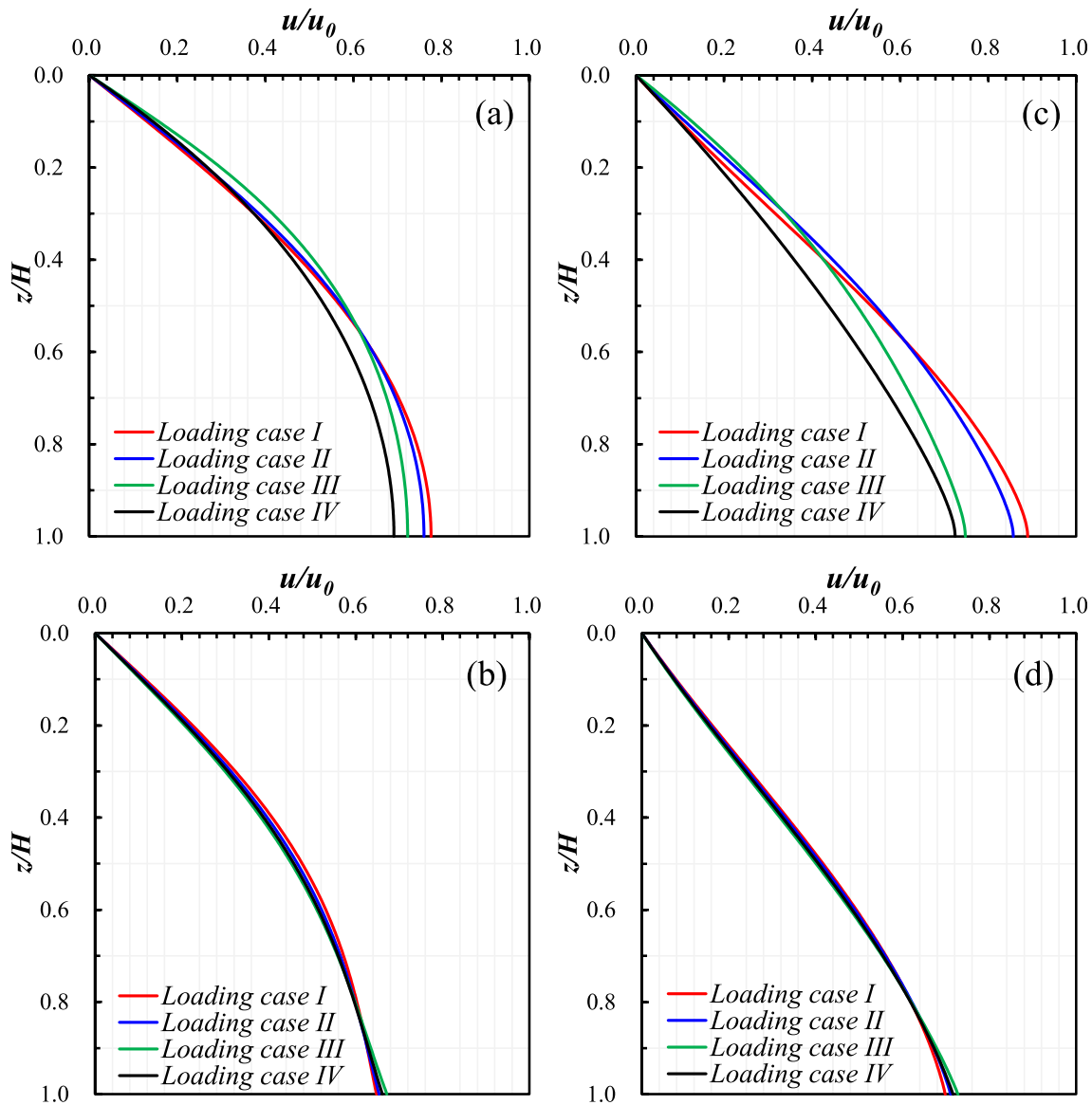


Fig. 17. Excess pore water pressure of 50% average degree under single drainage: (a) $p = q = 0$, (b) $p = 0, q = 1$, (c) $p = 1, q = 0$ and (d) $p = q = 1$.

would be the biggest value among them and the following one is the loading case II (the benchmark); the U_a of loading case III would be the smallest value, when do not consider depth variability in the sediment layer (i.e., $p = q = 0$). Firstly, it is indicated that instant thermal loading (loading case I) will lead to an over-assessment of U_a , which may result in optimistic judgements about the time required for sediment stability and pose a potential threat to subsequent project operations. Secondly, it is also shown that delaying the thermal loading time and prolonging the heating time would result in slower consolidation of the sediment layer, that is, the total consolidation time is prolonged accordingly. This is in line with the actual situation mentioned above. It is also worth noting that delaying the thermal loading time (loading case III) results in less value of U_a than prolonging the heating time (loading case IV), which means that delaying the thermal loading time has a more significantly prolonged effect than prolonging the heating time.

Fig. 14(b), (c) and (d) show the distributions of U_a with considering the depth variability (constant permeability, constant bulk modulus and constant C_v , respectively) in the sediment layer. The results also reveal the above-mentioned pattern, which means that considering depth variability does not play a significant role in the occurrence of the

prolonged effect on the consolidation caused by delaying the thermal loading time or prolonging the heating time.

By comparing four subplots of Fig. 14, it can be concluded that when depth variability (especially the depth variability of bulk modulus) is considered, it leads to a greater difference in U_a between loading case III (delaying the thermal loading time) and the benchmark (loading case II), that is, the consolidation time of loading case III will be prolonged to some extent.

Fig. 15 shows the distributions of u/u_0 of the sediment layer under double drainage with different loading cases. The result showed by Fig. 15 is consistent with the basic theory mentioned above that delaying the thermal loading time and prolonging the heating time would decrease the value of excess pore water pressure compared to the benchmark (loading case II). From Fig. 15, it is indicated that the maximum value of u/u_0 in loading case IV (prolonging the heating time) is the smallest one among these four loading cases and that the maximum value of u/u_0 in loading case I is the largest value. This means that the conventional assumption of instant loading would have over-estimated the value of excess pore water pressure.

Based on Figs. 14 and 15, loading case IV (prolonging the heating

time) seems to be the optimal loading case for both safety and economy under double drainage, since it has the smallest u/u_0 and only needs intermediate consolidation time.

4.2. Influence of different loading cases under single drainage

Fig. 16 shows the changes of average degree of thermal consolidation under single drainage with different loading cases. Basically, the distributions of U_a under single drainage reveals the same pattern with that under double drainage, which are that instant thermal loading (loading case I) will lead to an over-assessment of U_a ; the total consolidation time of loading case IV (prolonging the heating time) and loading case III (delaying the thermal loading time) would be longer than loading case II (the benchmark); and loading case III has a more significantly prolonged effect than loading case IV. However, the depth variability no longer has a great impact on the difference of these loading cases like that under double drainage.

Fig. 17 shows the distributions of u/u_0 of the sediment layer under single drainage with different loading cases. Fig. 17(a) and (c) show that the distribution of U_a under single drainage reveals the same pattern, that is, the maximum value of u/u_0 in loading case IV (prolonging the heating time) is the smallest one among these four loading cases. An interesting observation from Fig. 17(b) and (d) is that the distribution of u/u_0 at $U_a = 50\%$ is almost identical for different loading cases when the depth variability of bulk modulus is considered. This is mainly because when the depth variability of bulk modulus is considered, it would result in a great increase of the thermal excess pore water pressure u_{th} , especially at the bottom of the sediment layer, which leads to an increase in the proportion of u_{th} in the total excess pore water pressure; however, u at the bottom dissipates slowly under single drainage, so that the influence of q might not be significant, which would result in a situation where the distribution of u is approximately the same for different loading cases.

5. Conclusions

In this study, a new governing equation for thermal consolidation of saturated sediments is proposed by considering the depth variability of the sediment layer under the time-dependent loading, and the corresponding 1D analytical solution for thermal consolidation of saturated sediments is derived. The average degree of consolidation and the normalized excess pore water pressure in the saturated sediment layer at different depths and periods are calculated and compared in different cases by MATLAB. The validity of the proposed solution was demonstrated by comparing it with existing solutions. The main conclusions are as follows:

- (1) When T_v is less than T_{c2} (the starting time of thermal loading), the loading rate of the external force is proportional to the excess pore water pressure u , but this only affects the amplitude of u and does not affect the distribution of u with depth. It means that, without the thermal loading, the distribution of u with depth would show an inherent pattern.
- (2) The depth variability of bulk modulus has a greater effect on the distribution of U_a of thermally consolidated sediments relative to the depth variability of permeability. In comparison, the depth variability of permeability has a greater effect on the distribution of u/u_0 with depth relative to the depth variability of bulk modulus when $U_a = 50\%$.
- (3) For the distribution of u/u_0 under double drainage, the location of the maximum value of u/u_0 will move down with the increase of p . For the distribution of u/u_0 under single drainage, basically, the value of u/u_0 decreases with the increase of q for all depths; however, when only considering the depth variability of permeability, the distribution of u/u_0 in the bottom region of the sediment layer shows an opposite pattern.

- (4) Instant thermal loading will lead to an over-assessment of U_a , which may result in optimistic judgements about the time required for sediment stability and pose a potential threat to subsequent project operations. In addition, this conventional assumption of thermal loading would overestimate the value of excess pore water pressure.
- (5) Delaying the thermal loading time and prolonging the heating time would result in slower consolidation of the sediment layer. Normally, delaying the thermal loading time has a more significantly prolonged effect than prolonging the heating time and the maximum value of u/u_0 in prolonging the heating time is the smallest one. Therefore, prolonging the heating time may be the optimal option when considering both safety and economy.

Regarding the engineering feasibility of the analytical solution proposed in this study, it can be guaranteed that on the one hand it considers the construction and operation of the practical pipeline project and on the other hand the analytical solution is in a clear and mathematical form. The parameters involved in the analytical solution for thermal consolidation presented in this study can basically be obtained from laboratory tests. Parameters other than these, such as depth-dependent parameters, can be obtained from field tests, e.g., the distribution of void ratios of the soil layer with depth.

CRediT authorship contribution statement

Ming-Jun Hu: theoretical solution deviation, Methodology, Writing – original draft. **Wei-Qiang Feng:** Conceptualization, Methodology, Writing – review & editing, Supervision. **Jun Yang:** Formal analysis, Writing – review & editing.

Declaration of competing interest

The authors declare that they have no known competing financial interests or personal relationships that could have appeared to influence the work reported in this paper.

Data availability

Data will be made available on request.

Acknowledgements

We are thankful for the financial support given by the National Natural Science Foundation of China (Grant No. 52278356), Key Special Project for Introduced Talents Team of Southern Marine Science and Engineering Guangdong Laboratory (Guangzhou) (GML2019ZD0210), Project from Shenzhen Science and Technology Innovation Commission (JCYJ20210324105210028), the grand of Southern Marine Science and Engineering Guangdong Laboratory (Guangzhou) (K19313901).

References

- Abbasi, N., Rahimi, H., Javadi, A.A., Fakher, A., 2007. Finite difference approach for consolidation with variable compressibility and permeability. *Comput. Geotech.* 34 (1), 41–52.
- Bai, Y., Niedzwecki, J.M., 2014. Modeling deepwater seabed steady-state thermal fields around buried pipeline including trenching and backfill effects. *Comput. Geotech.* 61, 221–229.
- Cekerevac, C., Laloui, L., 2004. Experimental study of thermal effects on the mechanical behaviour of a clay. *Int. J. Numer. Anal. Methods GeoMech.* 28 (3), 209–228.
- Chatterjee, S., White, D.J., Randolph, M.F., 2013. Coupled consolidation analysis of pipe–soil interactions. *Can. Geotech. J.* 50 (6), 609–619.
- Cheng, Q., Yang, J., Li, Z., Tian, J., Gan, Y., Zhao, Y., 2020. Thermal–hydraulic coupling model and operating conditions analysis of waxy crude oil pipeline restart process after shutdown. *Adv. Mech. Eng.* 12 (2), 1687814020904256.
- Cui, C., Liang, Z., Xu, C., Xin, Y., Wang, B., 2023. Analytical solution for horizontal vibration of end-bearing single pile in radially heterogeneous saturated soil. *Appl. Math. Modell.* 116, 65–83.

- Cui, C.Y., Meng, K., Wu, Y.J., Chapman, D., Liang, Z.M., 2018. Dynamic response of pipe pile embedded in layered visco-elastic media with radial inhomogeneity under vertical excitation. *GeoMech. Eng.* 16 (6), 609–618.
- Cui, C., Meng, K., Xu, C., Wang, B., Xin, Y., 2022. Vertical vibration of a floating pile considering the incomplete bonding effect of the pile-soil interface. *Comput. Geotech.* 150, 104894.
- Delage, P., Sultan, N., Cui, Y.J., 2000. On the thermal consolidation of Boom clay. *Can. Geotech. J.* 37 (2), 343–354.
- Feng, J., Ni, P., Mei, G., 2019. One-dimensional self-weight consolidation with continuous drainage boundary conditions: solution and application to clay-drain reclamation. *Int. J. Numer. Anal. Methods GeoMech.* 43 (8), 1634–1652.
- Feng, W.Q., Yin, J.H., 2020. Development and verification of a new simplified method for calculating settlement of a thick soil layer with nonlinear compressibility and creep. *Int. J. GeoMech.* 20 (3), 04019184.
- Feng, W.Q., Zheng, X.C., Yin, J.H., Chen, W.B., Tan, D.Y., 2021. Case study on long-term ground settlement of reclamation project on clay deposits in Nansha of China. *Mar. Georesour. Geotechnol.* 39 (3), 372–387.
- Gashti, E.H.N., Uotinen, V.M., Kujala, K., 2014. Numerical modelling of thermal regimes in steel energy pile foundations: a case study. *Energy Build.* 69, 165–174.
- Hanna, D., Sivakugan, N., Lovisa, J., 2013. Simple approach to consolidation due to constant rate loading in clays. *Int. J. GeoMech.* 13 (2), 193–196.
- Indraratna, B., Kan, M.E., Potts, D., Rujikiatkamjorn, C., Sloan, S.W., 2016. Analytical solution and numerical simulation of vacuum consolidation by vertical drains beneath circular embankments. *Comput. Geotech.* 80, 83–96.
- Jiang, F., Dong, S., 2022. Two-level quantitative risk analysis of submarine pipelines from dropped objects considering pipe–soil interaction. *Ocean Eng.* 257, 111620.
- Jin, Z., Li, Z., Yin, Z.Y., Kotronis, P., 2021. Numerical modeling of soil–pipe interaction of single pipeline at shallow embedment in clay by hypoplastic macroelement. *Ocean Eng.* 241, 110017.
- Krost, K., Gourvenec, S.M., White, D.J., 2011. Consolidation around partially embedded seabed pipelines. *Geotechnique* 61 (2), 167–173.
- Li, J., Njock, P.G.A., Li, M.G., Chen, J.J., Xia, X.H., 2020. Consolidation responses of rheological aquitards to tide-induced groundwater fluctuations in coastal soft deposits. *Appl. Ocean Res.* 100, 102156.
- Liu, J.C., Shi, W.T., Lei, G.H., 2019. Influence of viscosity on one-dimensional thermal consolidation of marine clay. *Mar. Georesour. Geotechnol.* 37 (3), 331–338.
- Liu, X., El Naggar, M.H., Wang, K., Wu, W., 2021. Dynamic soil resistance to vertical vibration of pipe pile. *Ocean Eng.* 220, 108381.
- Mahmoud, M.S., Deresiewicz, H., 1980. Settlement of inhomogeneous consolidating soils—I: the single-drained layer under confined compression. *Int. J. Numer. Anal. Methods GeoMech.* 4 (1), 57–72.
- McCartney, J.S., Jafari, N.H., Hueckel, T., Sánchez, M., Vahedifard, F., 2019. Emerging thermal issues in geotechnical engineering. In: *Geotechnical Fundamentals for Addressing New World Challenges*. Springer, Cham, pp. 275–317.
- Norris, S., 2017. Radioactive waste confinement: clays in natural and engineered barriers—introduction. *Geological Society, London, Special Publications* 443 (1), 1–8.
- Özsisik, M.N., 1980. *Heat Conduction*. John Wiley and Sons, New York.
- Paaswell, R.E., 1967. Temperature effects on clay soil consolidation. *J. Soil Mech. Found Div.* 93 (3), 9–22.
- Poskitt, T.J., 1969. The consolidation of saturated clay with variable permeability and compressibility. *Geotechnique* 19 (2), 234–252.
- Schiffman, R.L., Gibson, R.E., 1964. Consolidation of nonhomogeneous clay layers. *J. Soil Mech. Found Div.* 90 (5), 1–30.
- Shahrokhbadi, S., Cao, T.D., Vahedifard, F., 2020. Thermal effects on hydromechanical response of seabed-supporting hydrocarbon pipelines. *Int. J. GeoMech.* 20 (1), 04019143.
- Shi, Y.M., Wang, N., Gao, F.P., Qi, W.G., Wang, J.Q., 2019. Physical modeling of the axial pipe-soil interaction for pipeline walking on a sloping sandy seabed. *Ocean Eng.* 178, 20–30.
- Wang, K.J., Wang, L.Z., Hong, Y., Shan, Z.G., Liu, H.C., Shen, K.M., 2022. Temperature effect on the axial behaviour of a pipeline buried in soft clay. *Mar. Georesour. Geotechnol.* 1–15.
- Ward, W.H., Samuels, S.G., Butler, M.E., 1959. Further studies of the properties of London clay. *Geotechnique* 9 (2), 33–58.
- Ward, W.H., Marsland, A., Samuels, S.G., 1965. Properties of the London clay at the Ashford common shaft: in-situ and undrained strength tests. *Geotechnique* 15 (4), 321–344.
- Wu, R.Q., Xie, K.H., Cheng, Y.F., 2009. Analytical theory for one-dimensional thermal consolidation of saturated soil under time-dependent loading. *J. Zhejiang Univ.* 43 (8), 1532–1537 (In Chinese).
- Xu, C., Chen, Q., Liang, L., Fan, X., 2018. Analysis of consolidation of a soil layer with depth-dependent parameters under time-dependent loadings. *European Journal of Environmental and Civil Engineering* 22 (Suppl. 1), s200–s212.
- Yang, G., Liu, Y., Che, P., 2022. Thermal consolidation of saturated silty clay considering different temperature paths: experimental study and constitutive modeling. *Int. J. GeoMech.* 22 (3), 04021293.
- Yi, J.T., Liu, F., Zhang, T.B., Qiu, Z.Z., Zhang, X.Y., 2021. Determination of the ultimate consolidation settlement of jack-up spudcan footings embedded in clays. *Ocean Eng.* 236, 109509.
- Zeinali, M.S., Abdelaziz, S.L., 2021. Thermal consolidation theory. *J. Geotech. Geoenviron. Eng.* 147 (1), 04020147.
- Zhang, Q., Fang, T., Ye, G., Liu, G., Wang, R., Tian, Y., 2021. Effect of sitting time on the breakout force of mat foundation on soft marine clay seabed. *Ocean Eng.* 234, 108770.
- Zhang, X., Kong, G., Li, H., Wang, L., Yang, Q., 2022. Thermal conductivity of marine sediments influenced by porosity and temperature in the South China Sea. *Ocean Eng.* 260, 111992.
- Zhao, K., Wang, Q., Chen, S., Zhuang, H., Chen, G., 2021. Dynamic response of pipelines in liquefiable seabed under nature loadings: waves and currents. *Ocean Eng.* 230, 109051.
- Zhu, G.F., Yin, J., 1999. Consolidation of double soil layers under depth-dependent ramp load. *Geotechnique* 49 (3), 415–421.
- Zhu, G.F., Yin, J.H., 2012. Analysis and mathematical solutions for consolidation of a soil layer with depth-dependent parameters under confined compression. *Int. J. GeoMech.* 12 (4), 451–461.
- Zhu, W., Yan, J., Yu, G., 2018. Vacuum preloading method for land reclamation using hydraulic filled slurry from the sea: a case study in coastal China. *Ocean Eng.* 152, 286–299.